Published in Phys. Rev. B 66, 165204 (2002).

Low-temperature scanning tunneling spectroscopy of n-type GaAs(110) surfaces

R. M. Feenstra*
Department of Physics, Carnegie Mellon University, Pittsburgh, Pennsylvania 15213, USA

G. Meyer†
Paul Drude Institut für Festkörperelektronik, Hausvogteiplatz 5-7, 10117 Berlin, Germany

F. Moresco and K. H. Rieder
Institut für Experimentalphysik, Freie Universität Berlin, Arnimallee 14, 14195 Berlin, Germany

Scanning tunneling spectroscopy is used to study n-type GaAs(110) surfaces at temperatures near 10 K. Spectral lines associated with surface accumulation layer states are observed. Near dopant atoms, three additional lines are seen in the spectra. These lines are identified with the donor states near the conduction band minimum (seen at different voltages for tunneling into and out of the states) and with a perturbed state of the accumulation layer.

PACS numbers: 73.20.Hb, 71.20.Nr, 61.16.Ch

I. INTRODUCTION

Studies employing scanning tunneling spectroscopy (STS) on GaAs(110) surfaces have played an important role in the development of the field of scanning tunneling microscopy (STM) [1,2]. Unlike surfaces such as Si(111)7×7 or Si(111)2×1 which are dominated by surface states [3–5], the (110) surface of GaAs and other III-V semiconductors do *not* have electronic states within the semiconductor band gap [6]. As such, STS studies reveal the band gap of the bulk semiconductor [2], and states induced by adsorbates and surface defects have been observed within the gap [7]. In addition, contributions to the tunnel current have been seen from the accumulation layer which forms on the surface for appropriate voltages between the probe-tip and sample. This accumulation layer contribution was clearly identified in early room-temperature (RT) studies where it was termed the "dopant-induced component" [1], and discrete accumulation layer states have been resolved in low-temperature (LT) spectra [8]. The magnetic field dependence of these accumulation layer states has recently been studied by STM and STS for InAs(110) surfaces, revealing a wealth of interesting phenomena [9].

In this work we report the results of our LT-STS studies on n-type GaAs(110) surfaces. We observe a number of discrete lines in the spectra arising from the accumulation layer at the surface. In addition, three new spectral lines are observed in the vicinity of near-surface dopant atoms. Based on a comparison of the sample-tip voltage at which these lines occur with the expected band bending profiles in the semiconductor, these additional lines are identified as arising from: (1) tunneling into donor states, when the Fermi-level of the probe-tip coincides with the conduction band (CB) minimum at the semiconductor surface, (2) tunneling out of donor states when the Fermi-level of the sample coincides with the CB minimum at the semiconductor surface, and (3) an accumulation layer state which is perturbed by the ionized dopant atoms. The latter feature is the same as previously identified near dopant atoms on InAs(110) surfaces [8], but the former two spectral features were *not* seen in that work due to the difference in tip-induced band bending profiles between InAs and GaAs, as further discussed in Section IV. Prior results for LT tunneling spectra near dopant atoms have been reported for GaAs(110) surfaces, but the spectral features observed there were identified only in nonspecific terms as localized states of the sample or tip [10].

II. EXPERIMENT

Gallium arsenide wafers were cleaved in ultra-high-vacuum (pressure of about 1×10^{-10} Torr) at room temperature, exposing a (110) crystal face. Within a few minutes after cleaving, the samples were cooled to about 50 K and were introduced into a liquid-He cryostat containing the home-built STM [11]. The temperature of the sample in the STM during the measurements reported here was 8–12 K. Probe-tips were formed prior to sample cleavage by making a controlled mechanical contact of the tip to a clean copper surface, thereby transferring copper atoms to the end of the tip. Metallic tips are reliably formed in this manner [12].

As noted by prior workers [8,10], use of degenerate (*i.e.* metallic at low temperature) semiconductor samples is necessary to ensure sufficient conductivity for the LT-STM experiments. For the present work the Si-doped GaAs wafers had a RT carrier concentration specified as $(2.0–2.6)\times10^{18}$ cm^{-3}, corresponding to a resistivity of $(1.4–1.7)\times10^{-3}$ ohm-cm. These values imply that the material is indeed degenerate [13].

STM images were acquired with constant current of typically 0.3 nA, and at various sample-tip voltages specified below. Spectra were acquired usually at constant sample-tip separation, using a voltage modulation of

10–20 mV and employing a lock-in amplifier to obtain the conductance dI/dV. For spectra extending over a large voltage range the technique of continuously varying sample-tip separation was used to ensure a large dynamic range, applying $s(V) = s_0 + a \mid V \mid$ with values of a of typically 1 Å/V. Normalization in those cases is done by computing the ratio of differential conductance dI/dV to total conductance I/V, where a broadening of 1.5 V is applied to I/V to form a suitable normalization quantity [2]. For acquiring spectra at specific spatial locations, an image is first acquired and displayed on the computer monitor, and the specific locations are then specified as points on that image. The spectra are thus acquired a few seconds or minutes after the image. With a typical drift rate of ≈ 1 Å per hour in the STM, the location of the spectra are accurate to better than 1 Å. This positioning accuracy is quite adequate for the present study.

III. RESULTS

Figure 1 shows a constant-current STM image of the n-GaAs(110) surface, acquired with sample voltage of +1.5 V (thus corresponding to electrons tunneling from the probe-tip into normally empty states of the sample). The corrugation of the 1×1 surface unit cell, measuring 5.65×4.00 Å, is clearly visible. In addition, dopant atoms are revealed by the presence of the region of raised corrugation, as labeled by (f)–(j) in Fig. 1. Such dopant atom features in STM images have been extensively studied in the past, at both RT [14–16] and LT [8,10,17–19]. Dopant atoms in the surface atomic plane and in subsurface planes are seen; dopants as deep as the 5th layer have been reported in both RT [14] and LT studies [10]. For the present experiment assuming that dopants as deep as the 5th layer are visible we obtain a dopant concentration of 5×10^{18} cm^{-3}, in reasonable agreement with the specified concentration of (2.0–2.6)×10^{18} cm^{-3}. In addition to dopant atoms, we also observe a few other features indicated by "V" and "R" in Fig. 1, and we associate these features with either surface defects such as vacancies [20,21] or residual surface contamination, respectively.

Tunneling spectra, acquired at a typical surface location (not near a defect) are shown in Fig. 2. Figure 2(a) shows a spectrum acquired over a large voltage range using the variable sample-tip separation method described in Section II. The CB and VB components in the conductance are clearly seen, and the band edge are marked in the spectrum. A band gap of 1.60±0.05 eV is observed. This can be compared with the expected LT band gap of GaAs of 1.52 eV [22]. Our result is slightly larger than expected; this discrepancy may result from effects of tip-induced band bending [23]. One distinct surface-state related feature is observed, at +0.72 V, similar to that seen in RT-spectra [2]. Figure 2(b) shows a spectrum acquired with constant sample-tip separation over a more limited voltage range, focusing on the band gap region. A number of discrete spectral lines are observed, as indicated by the dash marks on the spectrum. Below we present spectra acquired at specific surface locations, on and off dopant atoms, from which we can deduce the origin of these discrete spectral lines.

Figure 3 shows individual tunneling spectra acquired at the surface locations indicated in Fig. 1. Spectra (a)–(e) were acquired on bare surface locations far from any defects or dopant atoms. The spectra all look similar, with a few (generally three) discrete lines observed in the range −0.8 to −1.2 V. Occasionally the line nearest 0 V may have enhanced intensity [as in Fig. 3(c)], but we associate such a spectrum with the unintentional proximity of a dopant or defect atoms (as seen in Fig. 1, the location at which spectrum (c) was acquired is, in fact, somewhat close to a dopant atom). We believe that these discrete spectral lines observed far from dopant atoms arise from localized states associated with a surface accumulation layer, as further discussed in Section IV.

Spectra (f)–(j) in Fig. 3 were acquired at the location of dopant atoms. Three new spectral lines are visible in those spectra, labeled A, B, and C in Fig. 3(f). The first line, denoted A, occurs at positive sample voltages very near the onset of the CB component. The second line, denoted B, occurs at a negative voltage whose magnitude is nearly equal to the voltage position of the A line. The third line, denoted C, occurs at a negative voltage with magnitude slightly less than that of the accumulation layer spectral lines. In terms of its voltage position it is sometimes difficult to distinguish this line from those of the accumulation layer lines. However, we find that the line C *either* displays a clear voltage separation from the accumulation layer lines *or* it displays a clear enhancement in intensity compared to the accumulation layer lines, so in all cases we regard it as a distinct, new spectral feature.

Further information on the identity of the spectral features A–C associated with the dopant atoms can be obtained by examining their detailed spatial dependence, as shown in Figs. 4 and 5. The constant-current STM image of Fig. 4 shows a dopant atom, and a series of locations are marked at which spectra were acquired. Spectra shown in Fig. 5(a)–(e), acquired on or very near the dopant atom clearly show the extra lines A, B, and C. As a function of distance away from the dopant the lines A and B decay in intensity fairly rapidly, whereas the state C decays more slowly. (Actually, in this case, the line C is not so intense right at the dopant, and it grows somewhat in intensity with increasing separation before it decays. In the spectrum of Fig. 5(k) the lines A and B are totally gone and the line C has nearly completely decayed in intensity.

For a complete experimental investigation of the new spectral features associated with the dopant atoms, we have finally performed imaging of those features. Results of that sort are shown in Fig. 6. Figure 6(a) and (b) shows constant-current images of empty and filled

states respectively. The empty states appear as regions of enhanced state-density, associated with the attractive Coulomb interaction between the positive donor core and the CB electrons [14,24]. The filled states show a decreased state-density around the dopants arising from the repulsive interaction between the donor core and VB holes, with enhanced state-density in the immediate vicinity of the donor believed to be due to current from the dopant-induced component (accumulation layer) [25]. The resulting contrast is oscillatory, as seen in Fig. 6(b). (A similar oscillatory contrast has been demonstrated for charged oxygen atoms on GaAs(110) surfaces, and direct spectroscopic measurements demonstrated the competing effect of VB and dopant-induced current components [26]). Additional oscillations in the contrast have been observed in prior studies emplying conductance images, and those oscillations can be attributed to Friedel-type oscillations in the charge density of the accumulation layer [18]. Figures 6(c) and (d) show spectra acquired far from, and directly on, the dopant atom. The spectral lines A, B,and C are marked in Fig. 6(d), located at voltages of +0.37, −0.44, and −0.78 V, respectively.

Figures 6(e)–(j) show conductance images, acquired with constant tip-sample separation, at various sample-tip voltages. Images (f) and (h) were acquired at the voltages corresponding precisely to the location of the spectral lines C and B, respectively. The associated electronic states are both seen to have circular symmetry around the dopant atom, with state C extending considerably further away from the dopant core in agreement with the results of Fig. 5. Image (i) was acquired at a voltage located at the leading edge of the spectral line A. The associated electronic state is also seen to be circularly symmetric around the dopant atom and has similar lateral extent as that associated with line B. Finally, images (e), (g), and (j) were acquired at voltages far from the dopant related spectral lines. In this case the images reflect the sinuous landscape of potential fluctuation of the VB and CB edges [9]. (For image (e) these features appear to be quite circularly symmetric around the dopant atom, but this behavior is just a chance occurrence here; images with larger lateral extent reveal that this behavior does *not* persist about this or other dopant atoms). The role of potential fluctuations in the tunneling spectra is further discussed in the following section.

IV. DISCUSSION

In this section we discuss the origin of the discrete spectral lines observed within the band gap region in the LT spectra of the *n*-type GaAs(110) surfaces. To this end we employ simple 1-dimensional computations of the tip-induced band bending in the semiconductor, using precisely the same method described in Ref. [1]. We use a LT band gap of 1.52 eV for GaAs [22], and a doping density of 2×10^{18} cm^{-3} which is within the range specified by the wafer supplier (see Section II). Since this doping concentration corresponds to degenerate material, all electrons are placed in the CB, thereby yielding a Fermi-level position in the bulk semiconductor of 0.086 eV above the CB minimum. Other parameters in the computation are taken initially to have the same values as in Ref. [1], namely, sample-tip separation $s = 9$ Å, sample electron affinity $\chi = 4.07$ eV, and tip work function $\phi_m = 4.5$ eV. The results for the surface band bending ϕ as a function of sample-tip voltage are shown in Fig. 7. The regimes of accumulation ($V < -0.2$ V), depletion ($-0.2 < V < 2.2$ V) and inversion ($V > 2.2$ V) are apparent. As discussed in Ref. [1] it is doubtful that inversion is actually established in the semiconductor, although in any case for the results discussed below we are not concerned with this particular voltage regime.

Energy band profiles including semiconductor, vacuum, and probe-tip are pictured in Fig. 8 for a few choices of sample-tip voltages which turn out to be important in our discussion below. Those diagrams show the CB minimum of the sample together with the Fermi-levels of tip and sample. Note that the diagrams are drawn to scale in the horizontal (distance) and vertical (energy) axes, as indicated on the figure.

Let us first consider the band bending and tunnel current occurring for each situation picture in Fig. 8 assuming that the probe-tip is far from a dopant atom. Figure 8(a) shows the case of 0 V between sample and tip; since the work function of the tip is significantly larger than the electron affinity of the sample the semiconductor is therefore in depletion, as seen in the diagram. The surface bend bending is $\phi = 0.18$ eV. As the voltage is increased the semiconductor becomes more depleted, and a turn-on of the current occurs only when the tip Fermi-level is aligned with the CB minimum at the surface, as pictured in Fig. 8(b). The sample-tip voltage required for this situation is +0.20 V. At negative sample-tip voltages, current from the occupied CB states into the tip will be observed – the dopant-induced component [1]. This component turns on when the sample Fermi-level is aligned with the CB minimum at the surface, as pictured in Fig. 8(c). The sample-tip voltage required for that situation is −0.24 V. As the negative sample voltage grows, localized states will form in the accumulation layer which exists at the surface. Given a band bending profile $E_{CB}(x)$, the voltages at which localized states form can be estimated using the WKB approximation,

$$\int_{-\infty}^{0} k(x)dx + \frac{3\pi}{4} = \pi n \qquad (1)$$

with the semiconductor extending over $-\infty < x < 0$ and with $n = 1$ for the first state. In this equation,

$$k(x) = \sqrt{\frac{2m^*}{\hbar^2}(E - E_{CB}(x))} \qquad (2)$$

where $m^* = 0.067m_0$ [1], and to compute the voltage at which a localized state first forms we take $E =$

$E_{CB}(-\infty)$. The factor of $3\pi/4$ in Eq. (1) arises from the boundary conditions for the wave function, with $\pi/4$ coming from the left-side boundary within the semiconductor and $\pi/2$ from the right-side boundary of the vacuum-semiconductor interface. The latter is modeled here as an impenetrable barrier, although including the penetration of the wavefunction into the vacuum does not significantly change the result. We find that the first localized state forms for a surface band bending of $\phi = -0.067$ eV corresponding to a sample-tip voltage of -0.76 eV, as shown in Fig. 8(d). The formation of this state will contribute a discrete line to the tunneling spectrum, which in our 1D approximation corresponds to the bottom of a subband (*i.e.* with the electrons having momentum parallel to the surface). The second subband does not occur in the theory until a much larger value of the surface band bending, $\phi = 0.31$ eV, which occurs for a sample voltage of -1.78 V.

The results of the above computations for the position of features in the spectra acquired *far from* dopant atoms are in good agreement with the observations of Figs. 2–6. We can be confident that the parameters used in the computations are at least approximately correct since they predict an onset of the CB current of about $+0.2$ V, close to that observed experimentally. The discrete spectral lines observed at voltages less than about -0.8 V are in the correct location to correspond to the accumulation layer states expected from the theory. As mentioned in Section I, such features have been extensively studied for the case of InAs(110) [8,9], but for LT-STS studies of GaAs(110) only one prior work has been reported and the spectral features observed there were *not* specifically identified [10]. Curvature of the STM probe-tip will confine the accumulation layer states laterally, thereby changing the subband of a 1D model into a set of discrete state [8]. We attribute the splitting observed in the set of states near -0.8 V to this lateral quantization due to the tip.

An important distinction occurs in our present LT spectra of GaAs(110) compared to the prior LT results for InAs(110) [8]. The electron affinity of InAs is nearly 1 eV higher than that of GaAs [27]. Consequently, for a typical probe-tip the InAs surface is expected to be in accumulation even with zero volts between sample and tip; this expectation is confirmed by the experiments [8]. Therefore, in that case the ground state of the accumulation layer exists even when the tip Fermi-level is well *above* the state, so that applying negative sample-tip voltages causes the tip Fermi-level to scan through this state. The result is a relatively direct spectral measurement of the ground state. In contrast, for GaAs(110), the ground state of the accumulation layer is formed only when the tip Fermi-level is well *below* that state, as clearly seen in Fig. 8(d). The energy of the ground state is thus not simply related to the sample-tip voltage (*i.e.* it is *not* given by the usual expression of $eV + E_{Fs}$ where V is the sample-tip voltage and E_{Fs} is the sample Fermi-level). This situation is, of course, identical with that which occurs in RT spectra in which the broad accumulation layer component (*i.e.* the dopant-induced component) [1] occurs for n-type material at voltages corresponding to energies of $eV + E_{Fs}$ in the lower part of the gap, whereas the states themselves are actually positioned near the CB minimum.

Now let us consider the influence of a nearby dopant atom on the tunneling characteristics pictured in Fig. 8. The dopant atom will induce a localized state at an energy slightly below the semiconductor CB minimum [28]. Thus, at a voltage slightly less than that shown in Fig. 8(b) the tip Fermi-level will be aligned with that donor state, and a sharp spectral feature will result. We identify this feature with the line A observed in our spectra, *i.e.* the line A arises from from tunneling *into* the donor state. Similarly, at a voltage slightly smaller in magnitude than that shown in Fig. 8(c) the sample Fermi-level is aligned with the donor state and another sharp spectral feature results. We identify that feature with the state B observed in our spectra, *i.e.* arising from tunneling *out of* the donor states. Finally, for the case of the first accumulation layer state pictured in Fig. 8(d), the presence of a nearby donor atom will significantly perturb that state. The attractive potential of the donor will produce an accumulation layer state *lower* in energy than that pictured in Fig. 8(d), so that the state will be observed at negative sample-tip voltages with magnitude *less* than that of Fig. 8(d). We identify the perturbed state with the line C observed in our spectra. It is important to realize that, as described in the preceding paragraph, the voltages at which the lines B and C are observed are not simply related to the energy of the respective states. Rather, the states are located at energies well above the tip Fermi-level, and it is the alignment with the *sample* Fermi-level with the state as determined by the tip-induced band bending which determines the voltage position of the lines.

The above discussion provides, we believe, sufficient justification for our identification of the lines A and B as originating from tunneling into and out of, respectively, the surface donor states. However, it is informative to examine in more detail the position of these lines for different conditions in experiment and theory. Figure 9 shows computational results for the position of the A and B lines together with experimental results for those positions as observed on various dopant atoms and with two different probe-tips. The computational results are shown for several values of the doping concentrations. Along each theoretical line we vary the contact potential between tip and sample, defined as the difference between the tip work function and the electron affinity (the results of Fig. 8 discussed above were obtained with a contact potential of $4.5 - 4.07 = 0.43$ eV). We see that the observed points cluster reasonably well along the 2×10^{18} cm^{-3} doping density line, consistent with the specified doping for our samples. A change in contact potential between different probe-tips is not surprising since the tip work function will vary, but a less obvious implica-

tion from Fig. 9 is an apparently varying contact potential from one dopant atom to another as studied with the same probe-tip. We attribute this feature to potential fluctuations in the sample itself. For a random arrangement of dopant atoms with density 2×10^{18} cm^{-3} we expect those fluctuations to be on the order of 0.1 eV. The nearby presence of residual contaminants may increase this value, and small unintentional tip change may also lead to variations in the contact potential.

As seen in Fig. 9, observation of the A and B spectral lines associated with the near-surface dopant atoms provides a relatively sensitive means of determining doping density in the semiconductor, at least for large values of the probe-tip work function. A number of scanning probe methods for determining doping density already exist [29–31], but the technique illustrated in Fig. 9 provides a new and potentially useful method. Essentially, a determination of doping density using tunnel current involves two main unknown parameters: the doping density itself and the contact potential between tip and sample. By observing two spectral features, the A and B lines, we can determine both of these unknowns. Referring to Fig. 8, and placing for ease of discussion the sample Fermi-level right at the CB minimum, we see that the B line position corresponds to the voltage required to obtain flat band conditions in the semiconductor. This voltage thus essentially equals the contact potential difference between tip and sample, thereby determining that parameter. Using the additional information provided by the position of the A line, the doping density can be determined. We note that this technique for doping density determination is not restricted only to LT-STS measurements. Even at room temperature the dopant-induced (accumulation layer) component to the current is routinely observed; the onset of that component is basically the same as the location of the B line here, and the location of the CB component of the current is the same as the A line position. With a series of computations similar to those of Fig. 9, RT tunneling spectra of GaAs(110) surface can thus, in principle, be used to determine doping concentration of the GaAs.

Several parameters have not been explicitly considered in the above discussion. First, let us consider variations in the sample-tip separation. In constant-current images such as Fig. 1 this quantity varies typically by 0.5 Å due to changes in the state-density around the dopant atoms. We find that this variation in sample-tip separation plays a small role in determining results such those shown in Fig. 9. For example, reducing the sample-tip separation from 9 Å to 7 Å for the 2×10^{18} cm^{-3} line in Fig. 9 causes it to shift over and nearly fall on top of the 1×10^{18} cm^{-3} line. Thus, variations in sample-tip separation will produce an uncertainty in the doping density determination of less than a factor of 2. Second, we consider the effect of the depth of the dopant atom below the surface. Referring to Fig. 8, we see that the electrostatic potential in the semiconductor falls off relatively slowly, so that having a dopant atom at a depth of about 1 nm (4th atomic layer) below the surface will not lead to a significant shift in the observed line positions. Finally, we note that a quantitative understanding of tip-induced band bending must also include consideration of the probe-tip curvature, as discussed elsewhere [2]. The 3D nature of the probe-tip can reduce the tip-induced band bending by as much as a factor of two, and those effects will certainly modify theoretical results of the type presented in Fig. 9.

V. CONCLUSION

In summary, we have used STS at temperatures near 10 K to study cleaved n-type GaAs(110) surfaces. Spectroscopic features arising from an accumulation layer are observed, for negative sample-tip voltages. Near dopant atoms three new spectroscopic lines are seen. Based on computions of tip-induced band bending in the semiconductor, we identify these features as arising from tunneling into and out of the shallow donor state of the dopant, and from a perturbed state of the accumulation layer. Observation of the former two features is shown to provide a sensitive means of determined doping concentration, for the case when the tip work function is relatively large so that the tip-induced band bending is large.

VI. ACKNOWLEDGMENTS

This work was supported by a grant from the U.S. National Science Foundation (DMR-9985898) and by the E.U. TMR Project "Atomic/Molecular Manipulation". We thank F. Rose for useful discussions during the course of the experiments.

[1] R. M. Feenstra and J. A. Stroscio, J. Vac. Sci. Technol. B **5**, 923 (1987).
[2] R. M. Feenstra, Phys. Rev. B **50**, 4561 (1994).
[3] R. S. Becker, J. A. Golovchenko, D. R. Hamann, and B. S. Swartzentruber, Phys. Rev. Lett. **55**, 2032 (1985).
[4] R. J. Hamers, R. M. Tromp, and J. E. Demuth, Phys. Rev. Lett. **56**, 1972 (1986).
[5] J. A. Stroscio, R. M. Feenstra, and A. P. Fein, Phys. Rev. Lett. **57**, 2579 (1986).
[6] S. Y. Tong, A. R. Lubinsky, B. J. Mrstik, and M. A. Van Hove, Phys. Rev. B **17**, 3303 (1978).
[7] R. M. Feenstra, Phys. Rev. Lett. **63**, 1412 (1989).
[8] R. Dombrowski, Chr. Steinebach, Chr. Wittneven, M. Morgenstern, and R. Wiesendanger, Phys. Rev. B **59**, 8043 (1999).
[9] M. Morgenstern, Chr. Wittneven, R. Dombrowski, and R. Wiesendanger, Phys. Rev. Lett. **84**, 5588 (2000).

[10] A. Depuydt, C. Van Haaesendonck, N. S. Maslova, V. I. Panov, S. V. Savinov, and P. I. Arseev, Phys. Rev. B **60**, 2619 (1999).
[11] G. Meyer, Rev. Sci. Instrum. **67**, 2960 (1996).
[12] R. M. Feenstra, G. Meyer, F. Moresco, and K. H. Rieder, Phys. Rev. B **64**, 081306 (2001).
[13] J. Singh, *Physics of Semiconductors and their Heterostructures* (McGraw-Hill, New York, 1993), p. 272.
[14] M. B. Johnson, O. Albrektsen, R. M. Feenstra, and H. W. M. Salemink, Appl. Phys. Lett. **63**, 2923 (1993); **64**, 1454 (1994).
[15] J. F. Zheng, X. Liu, N. Newman, E. R. Weber, D. F. Ogletree, and M. Salmeron, Phys. Rev. Lett. **72**, 1490 (1994).
[16] C. Domke, Ph. Ebert, M. Heinrich, and K. Urban, Phys. Rev. B **54**, 10288 (1996).
[17] M. C. M. M. van der Wielen, A. J. A. van Roij, and H. van Kempen, Phys. Rev. Lett. **76**, 1075 (1996).
[18] Chr. Wittneven, R. Dombrowski, M. Morgenstern, and R. Wiesendanger, Phys. Rev. Lett. **81**, 5616 (1998).
[19] R. de Kort, M. C. M. M. van der Wielen, A. J. A. van Roij, W. Kets, and H. van Kempen, Phys. Rev. B **63**, 125336 (2001).
[20] G. Lengel, R. Wilkins, G. Brown, M. Weimer, J. Gryko, and R. E. Allen, Phys. Rev. Lett. **72**, 836 (1994).
[21] Ph. Ebert and K. Urban, Phys. Rev. B **58**, 1401 (1998).
[22] *Semiconductors: group IV elements and III-V compounds*, ed. O. Madelung, (Springer-Verlag, Berlin, 1991).
[23] At RT the effects of tip-induced band bending on the observed band gaps was found to be remarkably small (< 0.05 eV) for high doping values of the type used here, as discussed in Ref. [2]. However, we note that in the present LT spectra tip-induced band bending effects may be more apparent, since for the RT results both the VB and CB probably extend into the gap region by several kT thereby masking the effects of tip-induced band bending.
[24] J. A. Stroscio and R. M. Feenstra, J. Vac. Sci. Technol. B **6**, 1472 (1988).
[25] C. Domke, M. Heinrich, Ph. Ebert, and K. Urban, J. Vac. Sci. Technol. B **16**, 2825 (1998).
[26] J. A. Stroscio, R. M. Feenstra, and A. P. Fein, Phys. Rev. Lett. **16**, 1668 (1987).
[27] J. van Laar, A. Huijser, and T. L. van Rooy, J. Vac. Sci. Technol. **14**, 894 (1977).
[28] In bulk GaAs the ground state of a donor has binding energy of about 6 meV. Near the surface this binding energy will be increased by about a factor of 4 due to the reduced dielectric screening. However, the state itself will acquire p-like symmetry since it will be predominantly localized within the semiconductor, thus yielding a reduction in binding energy of about a factor of 4. We thus expect at the surface a ground state binding energy similar to that in the bulk.
[29] A. Schwarz, W. Allers, U. D. Schwarz, and R. Wiesendanger, Phys. Rev. B **62**, 13617 (2000).
[30] Y. Huang, C. C. Williams, and M. A. Wendman, J. Vac. Sci. Technol. A **14**, 1168 (1996).
[31] M. Barrett, M. Dennis, D. Tiffin, Y. Li, and C. K. Shih, IEEE Electron Dev. Lett. **16**, 118 (1995).

FIG. 1. Constant-current STM image of n-GaAs(110) surface, acquired at a sample voltage of +1.5 V. The gray scale range is 0.5 Å. Locations at which tunneling spectra were acquired are indicated by (a)–(k). Surface defects (probably vacancies) are indicated by "V" and residual surface contamination by "R".

FIG. 2. Typical tunneling spectra, acquired at nonspecific surface locations. (a) Large-range spectrum, acquired with varying sample-tip separation, and (b) spectrum of band gap region, acquired with fixed sample-tip separation. Discrete spectral lines observed in the gap region are indicated in (b). For sample states probed by the tip Fermi-level, the sample voltage corresponds to the energy of the state relative to the sample Fermi-level.

FIG. 3. Tunneling spectra acquired at the surface locations indicated in Fig. 1. Spectra (a)–(e) were acquired at locations far from dopant atoms, and spectra (f)–(j) were acquired directly on top of dopant atoms. Each spectrum is multiplied by the factor indicated prior to plotting, for ease of viewing. Successive spectra are shifted by one unit along the vertical axis. Discrete spectral lines observed at the dopant atoms are indicated by A, B, and C.

FIG. 4. Constant-current STM image of dopant atom, acquired with a sample voltage of +1.8 V and displayed with gray scale of 0.17 Å. Location at which spectra were acquired are indicated.

FIG. 5. Series of tunneling spectra acquired at the locations indicated in Fig. 4. Successive spectra are shifted by one unit along the vertical axis. Discrete spectral lines observed near the dopant atom are indicated by A, B, and C.

FIG. 6. (a) and (b): Constant-current STM images acquired at sample voltages of +1.5 and −2.2 V, respectively. Gray scale ranges are 0.5 and 0.2 Å, respectively. (c) and (d): Tunneling spectra acquired off and on the donor atom, respectively. (e)–(j): Conductance images, acquired at constant tip-height and at voltages of −1.0, −0.775, −0.60, −0.425, +0.35, and +0.60 V, respectively. All images are displayed with a gray scale in which low conductance is black and high conductance is white.

FIG. 7. Theoretical results for surface band bending, ϕ, as a function of sample-tip voltage. Computations are performed with tip work function $\phi_m = 4.5$ eV, sample electron affinity $\chi = 4.07$ eV, sample-tip separation of 9 Å, n-GaAs doping density of 2×10^{18} cm^{-3} and at a temperature of 10 K.

FIG. 8. Theoretical band profiles at energies near the Fermi-levels of the metal probe-tip and the semiconductor sample. Profiles are drawn to scale in both energy and distance. Case (a) shows the band profile for zero voltage between sample and tip. Cases (b)–(d) shows cases which correspond to the observed spectral lines A–C, respectively. The heavy line in case (d) indicates a localized accumulation layer state, just forming at that energy.

FIG. 9. Positions of the "A" and "B" spectral lines, as observed in experiment (open symbols, with each type of symbol corresponding to a different probe-tip) and computed from theory (lines and solid dots). Each theoretical line corresponds to a different doping density, as indicated, and along each line the contact potential between tip and sample is varied. The leftmost dot on each line corresponds to a contact potential of 0.43 eV and the rightmost dot to 0.73 eV.

Fig. 1

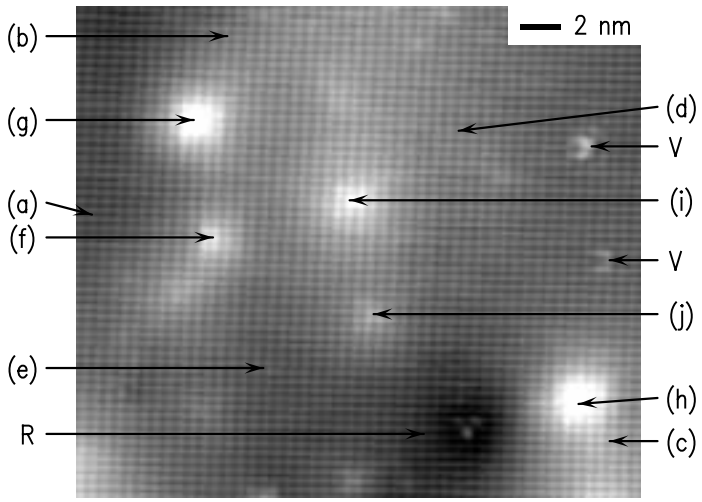

Fig. 2

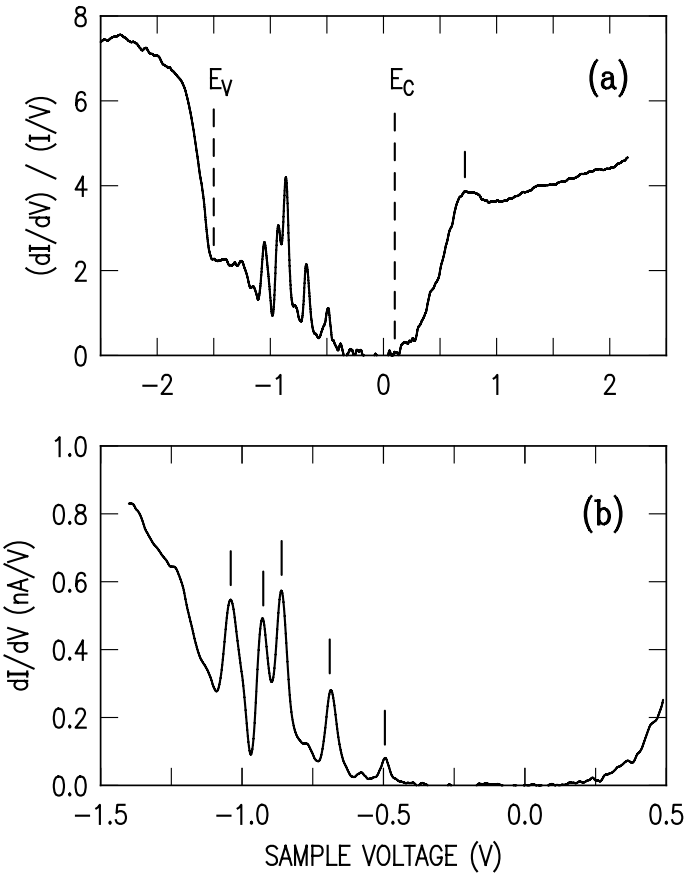

Fig. 3

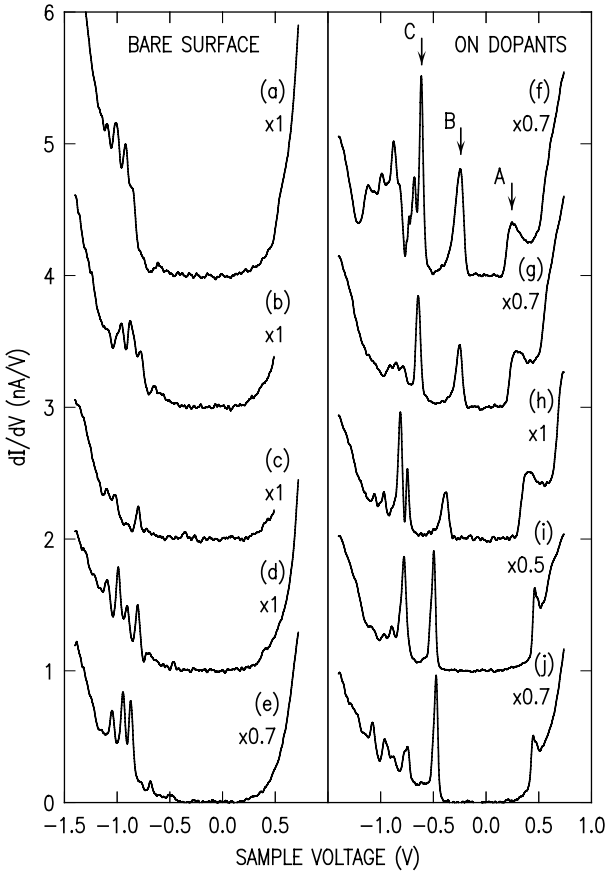
BARE SURFACE
ON DOPANTS
C
B
A
(a)
x1
(b)
x1
(c)
x1
(d)
x1
(e)
x0.7
(f)
x0.7
(g)
x0.7
(h)
x1
(i)
x0.5
(j)
x0.7
dI/dV (nA/V)
SAMPLE VOLTAGE (V)
0
1
2
3
4
5
6
−1.5 −1.0 −0.5 0.0 0.5
−1.0 −0.5 0.0 0.5 1.0

Fig. 4

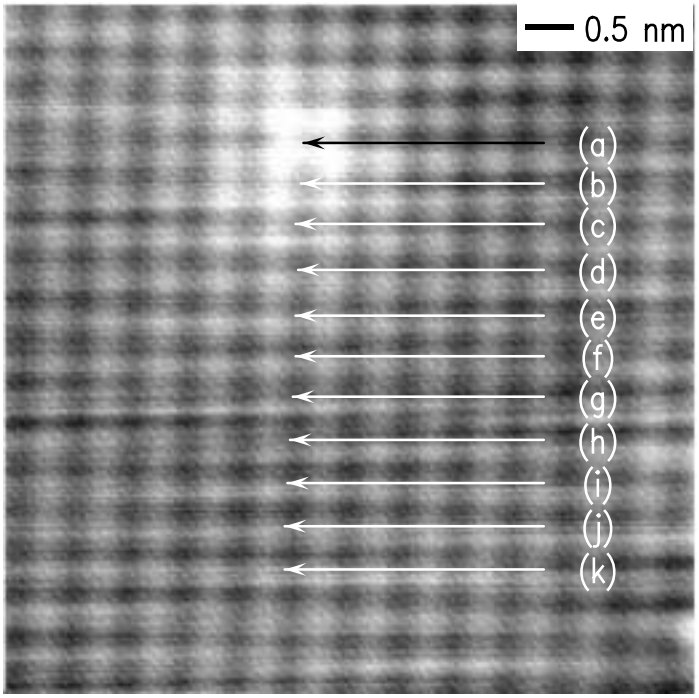
0.5 nm
(a)
(b)
(c)
(d)
(e)
(f)
(g)
(h)
(i)
(j)
(k)

Fig. 5

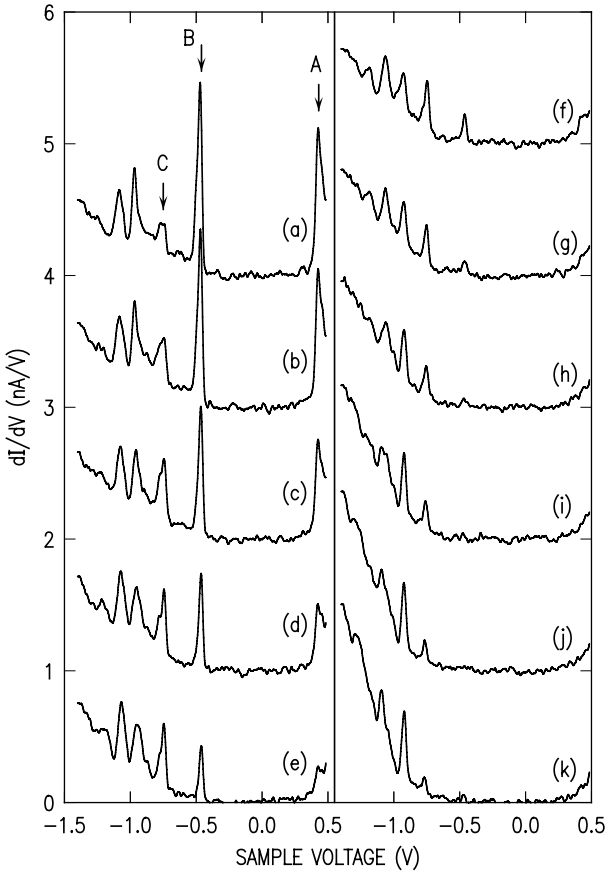
B
A
C
(a)
(b)
(c)
(d)
(e)
(f)
(g)
(h)
(i)
(j)
(k)
dI/dV (nA/V)
SAMPLE VOLTAGE (V)

Fig. 6

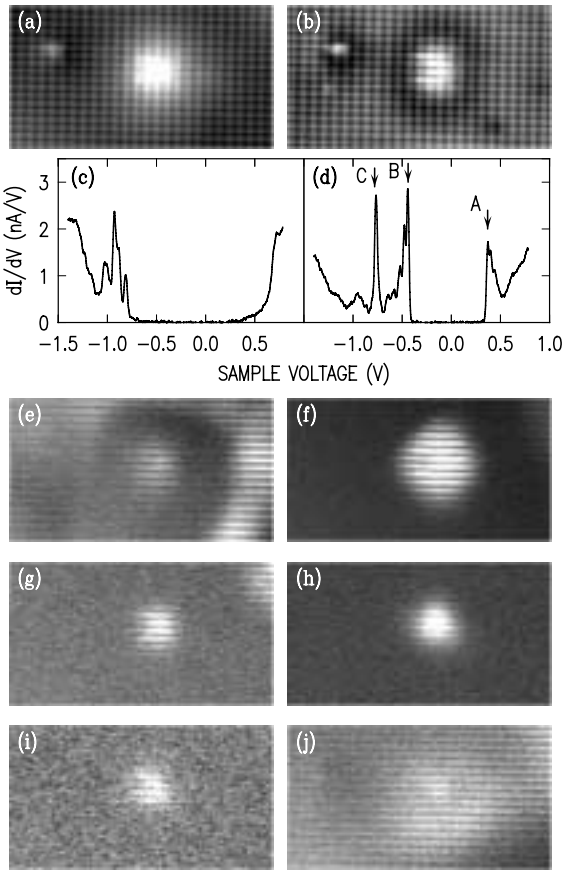
(a)
(b)
(c)
(d)
C
B
A
dI/dV (nA/V)
SAMPLE VOLTAGE (V)
(e)
(f)
(g)
(h)
(i)
(j)

Fig. 7

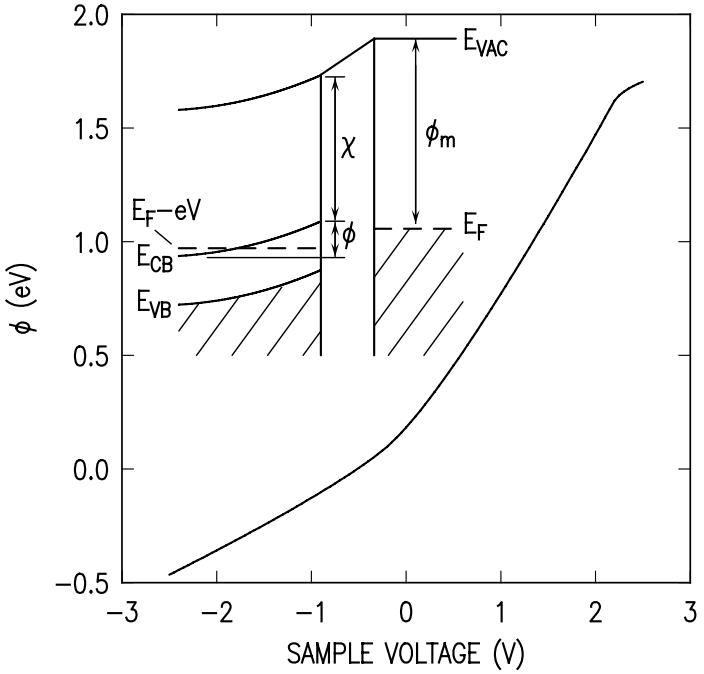
2.0
1.5
1.0
0.5
0.0
−0.5
−3
−2
−1
0
1
2
3
SAMPLE VOLTAGE (V)
ϕ (eV)
E_VAC
χ
ϕ_m
E_F−eV
E_CB
ϕ
E_F
E_VB

Fig. 8

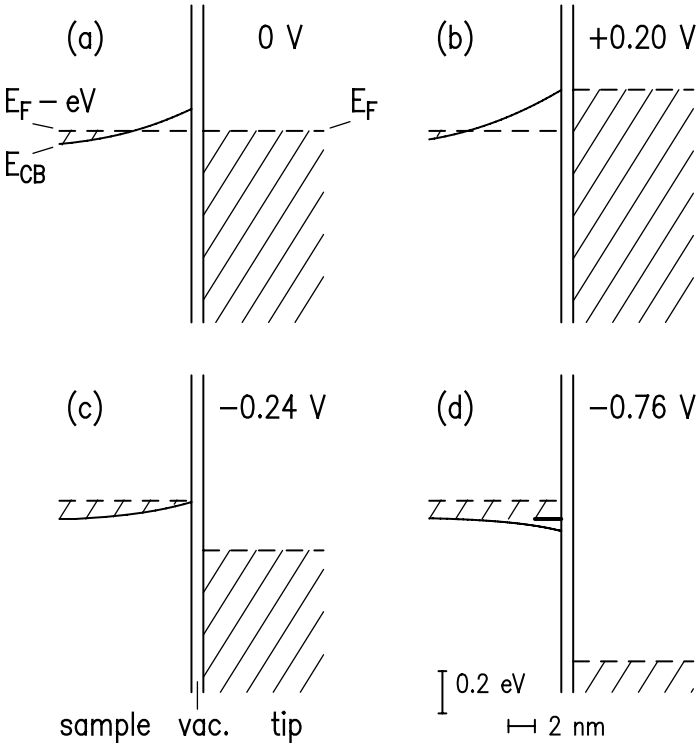
(a)
0 V
E_F − eV
E_F
E_CB
(b)
+0.20 V
(c)
−0.24 V
(d)
−0.76 V
sample
vac.
tip
0.2 eV
2 nm

Fig. 9

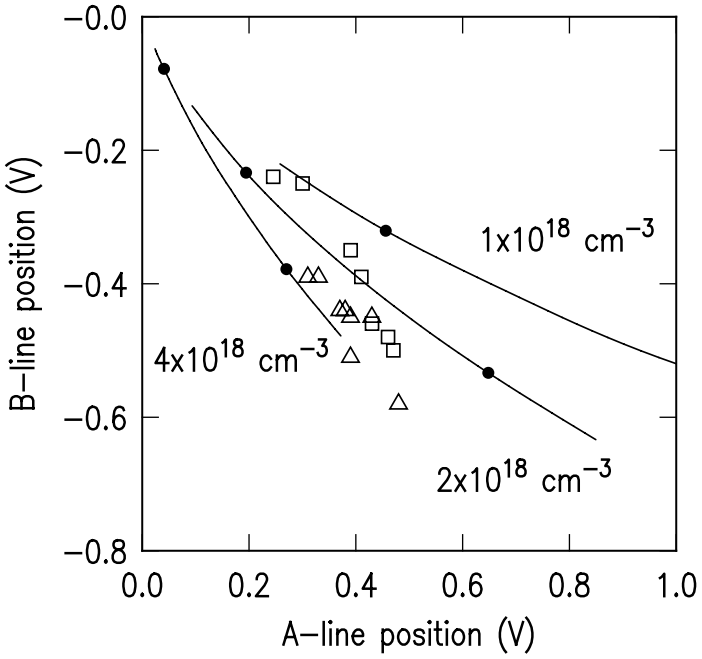
−0.0
−0.2
−0.4
−0.6
−0.8
0.0
0.2
0.4
0.6
0.8
1.0
B−line position (V)
A−line position (V)
1x10^18 cm^−3
4x10^18 cm^−3
2x10^18 cm^−3